Modelling and H1 force control of a nonlinear piezoelectric cantilever.

Micky Rakotondrabe, Yassine Haddab, Philippe Lutz

Modelling and H∞ force control of a nonlinear piezoelectric cantilever

Micky Rakotondrabe, Yassine Haddab and Philippe Lutz

***Abstract*— During a micromanipulation, it is important to have the same performances whatever the manipulated object is. We present in this paper the control of the force applied to flexible and rigid micro-objects by a piezoelectric cantilever. First, the voltage-force transfer function is modeled. The hysteresis and creep phenomena are taken into account. The reliance of the model on the characteristics of the micro-objects is clearly detailed. Then, in order to reject disturbances and maintain tracking performances required in micromanipulation, a H_∞ controller is designed. Finally, the experimental results end the paper.**

I. Introduction

Because of their high resolution and rapidity, piezoelectric materials are very used in micromanipulation. One of their applications is the piezoelectric microgripper which is made up of two piezoelectric cantilevers (example in [1]). During the micromanipulation, it is important to control the manipulation force because the micro-objects, notably biological and optical micro-objects, are often breakable. To perform that, the first piezoelectric cantilever is controlled on position while the second is controlled on force (Fig. 1). When the piezoelectric cantilevers work in large deflection, nonlinearities (hysteresis and creep) become non-negligible. They particularly appear in the voltage-deflection transfer function [2]. To reach the performances needed in micromanipulation, these nonlinearities must be taken into account. To model the creep, logarithmic functions [3] and linear operators [4] have been used. Furthermore, hysteresis has been modeled with the Preisach operator [5], the Maxwell operator [6], the polynomial approximation [7] and the variable-gain/variable-time-delay approximation [8]. These different models are enough accurate but some of them need high computing memory and power.

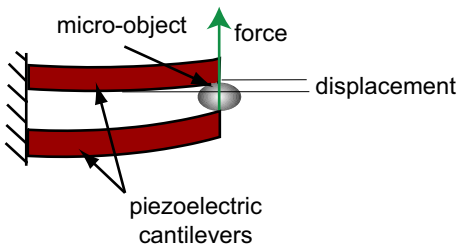

Fig. 1. A piezoelectric microgripper which manipulates a micro-object.

Laboratoire d'Automatique de Besançon
LAB CNRS UMR6596
ENSMM - Université de Franche-Comté
24, rue Alain Savary
25000 Besançon - France
{mrakoton,yhaddab,plutz}@ens2m.fr

The aim of this paper is the modelling and the control of the manipulation force applied to a micro-object by a piezoelectric cantilever. As the controller is dedicated to an embedded calculator, the simplicity of the model and of the controller is particularly taken into account. To modelize the hysteresis and the creep, the quadrilateral approximation is used because of its simplicity. In addition, the reliance of the final model on the characteristics of the manipulated micro-objects is demonstrated. Then, these characteristics are neglected and the uncertainty of the model is increased. As the model is subjected to uncertainty, we propose a H_∞ robust controller.

The paper is organized as follow. The second section is dedicated to the modelling. Then, the identification of the model is presented. The synthesis of the H_∞ controller is detailed in the fourth section. Finally the experimental results are presented in the last section.

II. Modelling the voltage-force transfer

This section presents the modelling of the transfer between the voltage U supplied to a piezoelectric cantilever and the force F_m that it applies to a manipulated micro-object (Fig. 2). According to *Smits and Choi* [9], the relation between the voltage U, the force F applied at the tip of the cantilever and the resulting deflection δ in the static phase is affine:

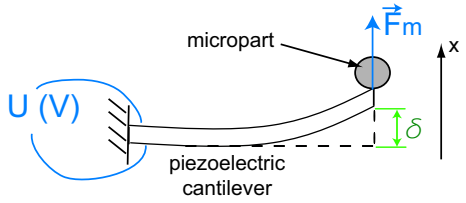

Fig. 2. A piezoelectric cantilever.

$$\delta = s_p \cdot F + d_p \cdot U \tag{1}$$

where $s_p > 0$ is the elastic constant of the cantilever and $d_p > 0$ is the piezoelectric constant.

In our previous work [1], it has been shown that the transient part of the (U, δ)-transfer and the transient part of the (F, δ)-transfer are similar. Thus, we have:

$$\delta = (s_p \cdot F + d_p \cdot U) \cdot D(s) \tag{2}$$

where $D(s)$ (with $D(0) = 1$) represents the dynamic part and s the Laplace variable.

However, when the deflexion δ of the cantilever becomes large, generally higher than 15% of the maximum field strength [11], the linear modelling is not applicable anymore and hysteresis and creep phenomena arise (Fig. 3). The creep is defined as a drift of the deflection after the end of the transient part. Let $\psi(.)$ be a nonlinear

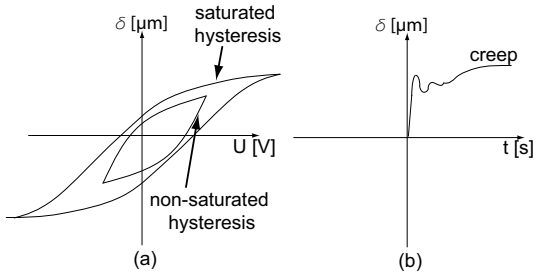

Fig. 3. a: hysteresis phenomenon. b: creep phenomenon.

operator taking into account the hysteresis, the creep and the dynamic part $D(s)$. From the (Equa. 2), we have:

$$\delta = s_p \cdot F \cdot D(s) + \psi(U) \tag{3}$$

In the sequel, we focus on the manipulation force $F_m = -F$. For all the theoretical analyses, the cantilever is supposed to be in contact with the manipulated micro-object. Fig. 4 presents the experimental setup. A unimorph piezoelectric cantilever has been used. Its sizes are: $15mm \times 2mm \times 0.3mm$ (length, width and thickness).

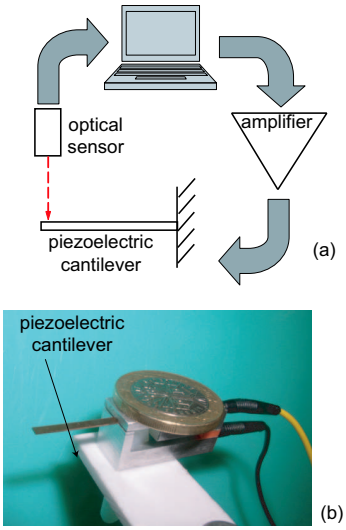

Fig. 4. a: the experimental setup principle. b: photography of the piezoelectric cantilever.

A. Nonlinear model

Fig. 5 represents the cantilever in contact with a micro-object. A sufficient model of the micro-object is composed of an effective mass m_e, a viscous damper c_e

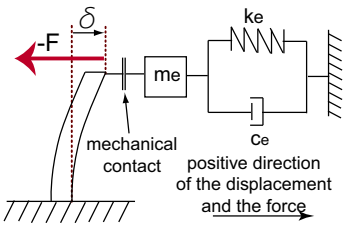

Fig. 5. A piezoelectric cantilever in contact with a micro-object.

and a stiffness k_e [12]. From the Fig. 5 and the (Equa. 3), we have:

$$\begin{cases} \delta = s_p \cdot F \cdot D(s) + \psi(U) \\ \delta = -s_e \cdot F \cdot D_e(s) \\ F_m = -F \end{cases} \tag{4}$$

where, $D_e(s)$ is the dynamic part of the micro-object and:

$$\begin{cases} D_e = \frac{1}{\frac{m_e}{k_e} \cdot s^2 + \frac{c_e}{k_e} \cdot s + 1} \\ \\ s_e = \frac{1}{k_e} \end{cases} \tag{5}$$

Using the three equations of (Equa. 4), we infer the expression of the force applied to the micro-object:

$$F_m = \frac{1}{(s_e + s_p)} \cdot \psi(U) \cdot \frac{1}{\left(\frac{s_e \cdot D_e(s) + s_p \cdot D(s)}{(s_e + s_p)}\right)} \tag{6}$$

with:

$$\frac{(s_e \cdot D_e(0) + s_p \cdot D(0))}{(s_e + s_p)} = 1 \tag{7}$$

On the one hand, the model depends on the characteristics of the micro-object:

- when there is no manipulated micro-object, the parameters m_e, c_e and k_e are null. Then, according to the (Equa. 6), the force tends towards zero.
- however, when the micro-object is infinitely rigid (infinite values of k_e and c_e), the (Equa. 6) becomes the expression of a piezoelectric cantilever with a null bending.

To clearly show the reliance of the voltage-force model on the micro-object characteristics, experiments were done with a very flexible and a very rigid micro-objects. The experiments were done with only one piezoelectric cantilever as shown in Fig. 5. Fig. 6 shows the results obtained with harmonic experiments. These curves were compared with the dynamic characteristic $D(s)$ of the cantilever whose the static gain has been scaled to allow the comparison. The difference between the curves confirms that the voltage-force transfer depends on the micro-object characteristics. In addition, the transient part of the voltage-force transfer is different from the transient part of the voltage-deflection transfer. On the other hand, the relation between the applied voltage U and the manipulation force F_m is nonlinear because of the hysteresis and the creep phenomena inside the operator $\psi(U)$. Fig. 7 is an experimental result illustrating that there is a creep on the measured force

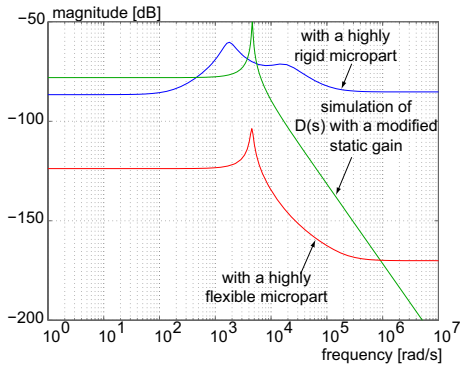

Fig. 6. Harmonic characteristics of the voltage-force transfer.

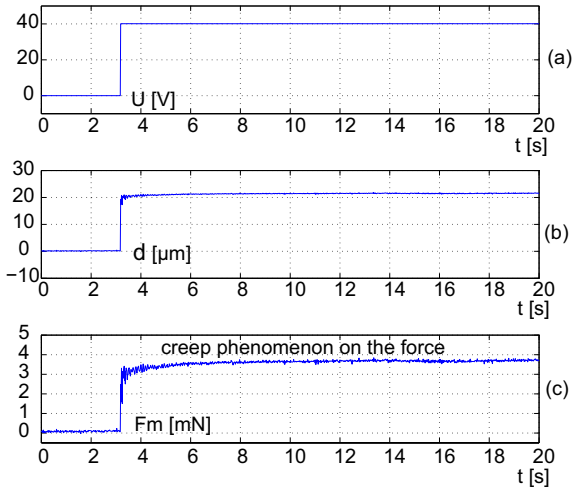

Fig. 7. Creep of the resulting force when a step voltage is applied.

when a step voltage is applied. In the following subsection, we model the nonlinear operator $\psi(U)$ using the quadrilateral approximation. We have demonstrated the relevance of this approximation in our previous work [10]. This approximation infers a linear model. In such approximation, the hysteresis infers an uncertainty while the creep infers a disturbance. The parameters are easy to identify and the simplicity of the model leads to low memory and time consuming controllers which are appropriate for embedded systems.

B. Quadrilateral approximation of ψ

Let $\delta = \psi(U)$ be the relation between the applied voltage and the resulting deflection when the force is null. It contains the hysteresis and the creep.

The hysteresis on the (U, δ)-plane can be approximated by a plurilinear curves, i.e. affine curve piecewise (Fig. 8-a). Let (Δ) be a variable straightline. Because the latter represents a hysteresis, its offset δ_0 and its slope α are dependent on the past and present values of input U. We note them $\delta_{U0}(.)$ and $\alpha(.)$. Thus, the approximation model of the hysteresis using the variable straightline is:

$$(\Delta) \quad : \quad \delta(s) = \alpha(.) \cdot U(s) + \delta_{U0}(.) \tag{8}$$

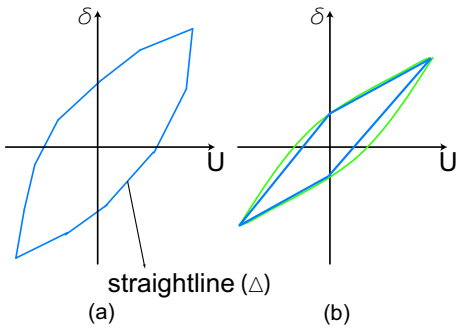

Fig. 8. a: plurilinear approximation of a hysteresis. b: quadrilateral approximation.

When the hysteresis does not have a saturation, a quadrilateral approximation is sufficient (Fig. 8-b). Let (Δ_M) and (Δ_m) represent the two straightlines of the quadrilater with respectively the maximal and the minimal slopes:

$$\begin{cases} (\Delta_M): & \delta(s) = \alpha_M \cdot U(s) + \delta_M(.) \\ (\Delta_m): & \delta(s) = \alpha_m \cdot U(s) + \delta_m(.) \end{cases} \tag{9}$$

where α_M (respectively α_m) represents the maximal (respectively minimal) slope and $\delta_M(.)$ (respectively $\delta_m(.)$) represents the corresponding offset.

Let α_O be the middle value of the maximal and the minimal slopes and let α_E be their radius:

$$\begin{cases} \alpha_O = \frac{\alpha_M + \alpha_m}{2} \\ \alpha_E = \frac{\alpha_M - \alpha_m}{2} \end{cases} \tag{10}$$

So, to model the hysteresis, we propose to use one nominal straightline with a nominal slope and a new offset $\delta_{h0}(.)$:

$$\delta(s) = \alpha_O \cdot U(s) + \delta_{h0}(.) \tag{11}$$

Here, the static gain α_O is subjected to uncertainty while δ_{h0} represents a disturbance.

To introduce the creep, we propose to consider it as an error due to a fictive time-variant force F_C. The new model which includes the hysteresis and creep effects is:

$$\delta(s) = \alpha_O \cdot U(s) + \delta_{h0} + s_C \cdot F_C(s) \tag{12}$$

where s_C is the fictive elastic constant.

Finally, we have:

$$\delta(s) = \alpha_O \cdot U(s) + \delta_0 \tag{13}$$

with $\delta_0 = \delta_{h0} + s_C \cdot F_C(s)$ is a disturbance to reject.

The (Equa. 13) represents the static modelling of the voltage-deflection transfer. Two comments can be arised:

- when the hysteresis phenomenon is weak, we have $\alpha_O = d_p$,
- as the creep was represented by the effect of a fictive force, the dynamic characteristic of the creep-deflection transfer and the dynamic characteristic of the force-deflection transfer are similar.

From the precedent two remarks and using the dynamic part of the (Equa. 2), we obtain the dynamic model between the voltage and the deflection:

$$\delta(s) = \psi(U) = (\alpha_O \cdot U(s) + \delta_0) \cdot D(s) \tag{14}$$

C. The nominal model

From the nonlinear model of force in (Equa. 6) and the quadrilateral approximation of $\psi(U)$ in (Equa. 14), we have:

$$\begin{aligned} F_m = & \frac{\alpha_O}{(s_e+s_p)} \cdot U(s) \cdot D(s) \left(\frac{s_e \cdot D_e(s) + s_p \cdot D(s)}{(s_e+s_p)} \right)^{-1} \\ & + F_{dist} \cdot D(s) \cdot \left(\frac{s_e \cdot D_e(s) + s_p \cdot D(s)}{(s_e+s_p)} \right)^{-1} \end{aligned} \tag{15}$$

where the disturbance is represented by:

$$F_{dist} = \frac{\delta_0}{(s_e + s_p)} \tag{16}$$

We notice that the model depends on the parameters s_e and D_e of the micro-object. It is not useful to identify the model and to synthesize a controller at each change of manipulated micro-object. Thus, we neglect these parameters and rely the closed-loop performances on the robustness of the controller. We use:

$$\begin{cases} s_e = 0 \\ \left(\frac{s_e \cdot D_e(s) + s_p \cdot D(s)}{(s_e+s_p)} \right)^{-1} = 1 \end{cases} \tag{17}$$

Using the (Equa. 16) and taking into account the (Equa. 17), the nominal model which represents the transfer between the applied voltage U and the manipulation force F_m is:

$$F_m = \frac{\alpha_O}{s_p} \cdot U(s) \cdot D(s) + F_{dist} \cdot D(s) \tag{18}$$

In this model, F_{dist} is a disturbance to be rejected. It contains the creep phenomenon and a part of the hysteresis (offset of the quadrilateral approximation). The static gain $\frac{\alpha_O}{s_p}$ is subjected to uncertainty and is defined by the (Equa. 10). The Fig. 9 shows the systemic scheme of the nominal model.

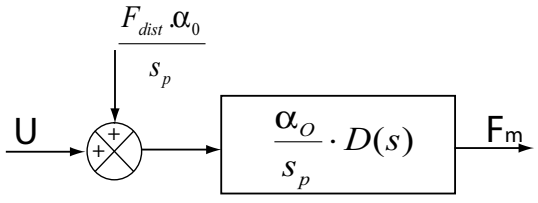

Fig. 9. Systemic scheme of the voltage-force transfer.

III. Identification

A. Piezoelectric gain identification

The first identification consists in identifying the parameter α_O. For that, a sine voltage U is applied to the piezoelectric cantilever and the resulting deflection δ is measured. A very low frequency ($f = 0.1Hz$) has been used in order to avoid the effect of the dynamic part on the hysteresis. The corresponding (U, δ)-curve is presented in the Fig. 10. From the curve and using the (Equa. 10), we easily deduct $\alpha_O = 502 \times 10^{-9} \left[\frac{m}{V}\right]$ and $\alpha_E = 64 \times 10^{-9} \left[\frac{m}{V}\right]$.

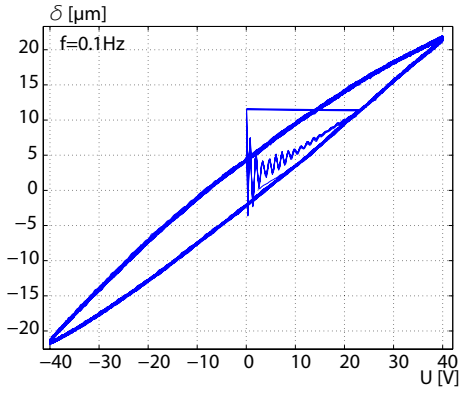

Fig. 10. The hysteresis in the (U, δ)-curve.

B. Elastic gain identification

Here, we want to identify the parameter s_p. For that, the electrodes are short-circuited in order to maintain the voltage U equal to zero. A weight ($= 20.72mN$) is hung on at the tip of the cantilever. The Fig. 11 shows the resulting deflection. From the results, we have $s_p = \frac{\delta}{F} = 1.931 \left[\frac{\mu m}{mN}\right]$.

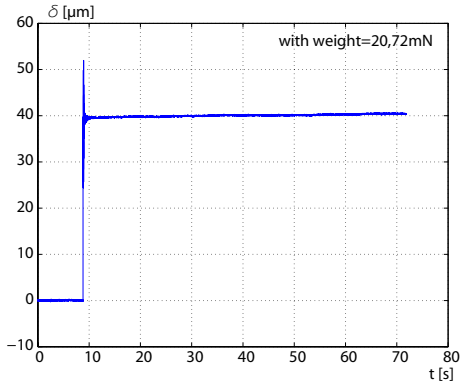

Fig. 11. The resulting deflection when a weight is hung on at the tip of the cantilever.

C. Dynamic part identification

In most cases, a second order model can sufficiently model the dynamic part of piezoelectric cantilevers [10][13]. It has the following form:

$$D(s) = \frac{1}{a \cdot s^2 + b \cdot s + 1} \tag{19}$$

where a is an inertial parameter and b a viscous parameter.

To identify $D(s)$, a step voltage is applied to the cantilever. The Fig. 12-(solid line) shows the resulting deflection. Using a curve fitting method, we have $a =$

4.722×10^{-8} and $b = 1.304 \times 10^{-5}$. The simulation of $D(s) \cdot \alpha_O$ is represented by the Fig. 12-(dashed plot).

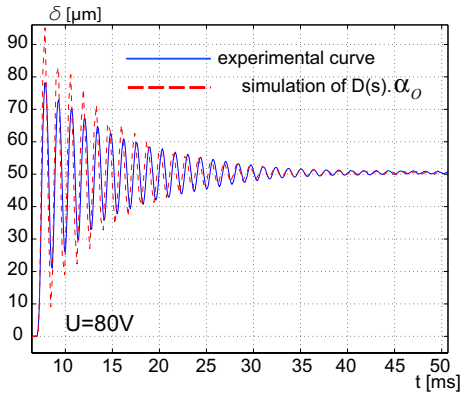

Fig. 12. The resulting deflection when a step voltage is applied to the cantilever.

IV. H_∞ CONTROL

On the one hand, the nominal model $G(s)$ is subjected to uncertainty due to the quadrilateral approximation. On the other hand, the parameters related to the micro-object have been neglected inside the model. Because of those approximations, we propose to use a H_∞ robust controller. The objective is to reject the disturbances in preserving tracking performances required in micromanipulation. For that, we use two weighting transfer functions W_1 and W_2 as shown in the Fig. 13. In this figure, F_{mc} represents the reference point of the manipulation force and $b = \frac{F_{dist} \cdot \alpha_O}{s_p}$.

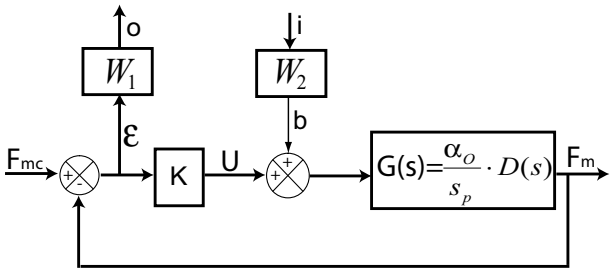

Fig. 13. The closed-loop scheme with the weighting functions.

A. Standard form

Let $P(s)$ be the augmented system including the nominal system and the weighting functions. The Fig. 14 shows the corresponding standard scheme. The standard H_∞ problem consists in finding an optimal value $\gamma > 0$ and a controller $K(s)$ stabilizing the closed-loop scheme of the Fig. 14 and guaranteeing the following inequality [14]:

$$\|F_l(P(s), K(s))\|_\infty < \gamma \tag{20}$$

where $F_l(.,.)$ is the lower Linear Fractionar Transformation and is defined by $F_l(P(s), K(s)) = \frac{o(s)}{e(s)}$.

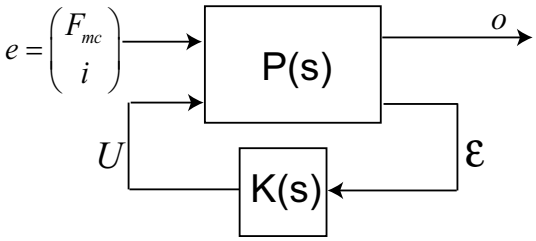

Fig. 14. The standard form.

From the Fig. 13, we have:

$$o = W_1 \cdot S \cdot F_{mc} - W_1 \cdot S \cdot G \cdot W_2 \cdot i \tag{21}$$

where $S = (1 + K \cdot G)^{-1}$ is the sensitivity function.

Using the condition (Inequa. 20) and the (Equa. 21), we infer:

$$\begin{array}{c} \|W_1 \cdot S\|_\infty < \gamma \\ \|W_1 \cdot S \cdot G \cdot W_2\|_\infty < \gamma \end{array} \Leftrightarrow \begin{array}{c} |S| < \frac{\gamma}{|W_1|} \\ |S \cdot G| < \frac{\gamma}{|W_1 \cdot W_2|} \end{array} \tag{22}$$

To solve the problem (Equa. 22), we use the Glover-Doyle algorithm which is based on the Riccati equations [15][16]. The issued controller K is robust in the fact that it ensures the stability and the performances even if the nominal system G has an uncertainty relative to the real plant. The wanted performances are introduced through the weighting functions.

B. Choice of the weighting functions

The transfer functions $\frac{1}{W_1}$ and $\frac{1}{W_1 \cdot W_2}$ are chosen from the specifications respectively on the tracking performances and on the disturbance rejection. The weighting functions W_1 and W_2 are automatically deduced. The specifications are:

- the maximal response time must be inferior to $10ms$,
- the overshoot must be null,
- the maximal statical error must be inferior to 0.1%,
- finally, the rejection of the disturbance is a lowpass filter with a cut frequency equal to $160Hz$.

From the above specifications, we choose:

$$\begin{array}{l} \frac{1}{W_1} = 10^{-3} \cdot \frac{3 \cdot s + 1}{3 \times 10^{-3} \cdot s + 1} \\ \\ \frac{1}{W_1 \cdot W_2} = 10^{-2} \cdot \frac{0.1 \cdot s + 1}{10^{-3} \cdot s + 1} \end{array} \tag{23}$$

C. Calculation of the controller

The computed controller has an order of 5. In order to minimize the memory and time consumptions in the computer, the controller order has been reduced to 3 using the balanced realization technique [17]. We obtain:

$$\begin{cases} K = \frac{2 \times 10^{-7} \cdot (s + 2.7 \times 10^{15}) \cdot (s^2 + 344 \cdot s + 2.5 \times 10^7)}{(s + 0.3) \cdot (s^2 + 2.1 \times 10^5 \cdot s + 1.2 \times 10^{10})} \\ \\ \gamma = 1.04 \end{cases} \tag{24}$$

V. Experimental results

The controller has been implemented in a PC-DSpace setup through the Simulink-Matlab software. The first experiment consists in analyzing the temporal performances of the closed-loop system. A step reference of $8mN$ amplitude has been applied. The analyses were performed for two different manipulated micro-objects (highly flexible and highly rigid micro-objects). The results (Fig. 15) show that the performances are maintained for both. The response time is nearly $10ms$ while the overshoot is null. In the second experiment, we

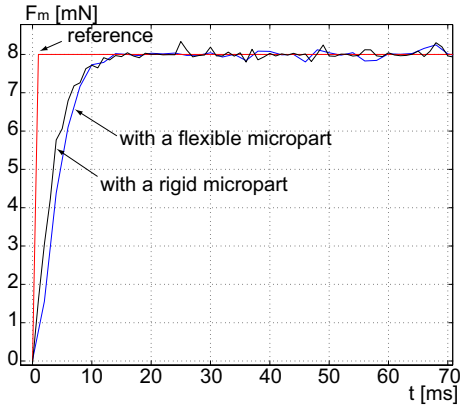

Fig. 15. Temporal analysis of the force control.

analyze the performances in the frequential domain. The frequential domain analysis is more concise than the temporal domain analysis. For that, a sine reference signal F_{mc} is applied and the resulting output F_m is measured. The corresponding magnitude is presented in the Fig. 16. The results clearly show that whatever the characteristics of the micro-object are, the H_∞ controller gives the same performances.

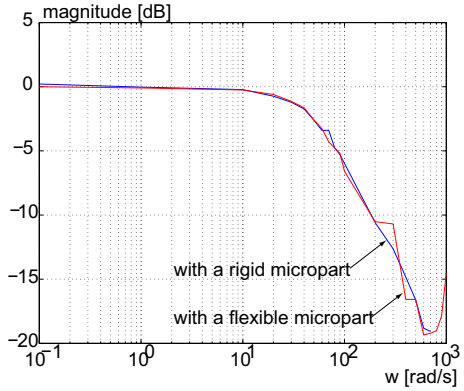

Fig. 16. Frequential analysis of the force control.

VI. Conclusion

In micromanipulation, the control of the force applied to the manipulated micro-object is important. This allows avoiding the destruction of the micro-object. This paper has presented the modelling and the control of force applied by a piezoelectric cantilever to micro-objects. The nonlinearities, i.e. hysteresis and creep phenomena, have been taken into account by using the quadrilateral approximation. Such approximation leads to a linear model under an uncertainty and a disturbance. Afterwards, a H_∞ controller has been designed. Finally, the experimental results have shown that whatever the manipulated micro-object is, the controller always gives good performances.

Acknowledgment

This work is partially supported by the European Project EUPASS (http://www.eupass.org/).

References

[1] Y. Haddab, N. Chaillet, A. Bourjault, 'A microgripper using smart piezoelectric actuators', IEEE/RSJ IROS, 2000.

[2] J. L. Pons, 'Emerging actuator technology: a micromechatronic approach', Wiley, ISBN: 0-470-09197-5, 2005.

[3] H. Jung, J.Y. Shim and D. Gweon, 'New open-loop actuating method of piezoelectric actuators for removing hysteresis and creep', REVIEW OF SCIENTIFIC INSTRUMENTS, 2000.

[4] K. Kuhnen and H. Janocha, 'Modeling of transfer characteristic of piezoelectric transducers by creep and hysteresis operators'.

[5] R.B. Mrad and H. Hu, 'A model for voltage to displacement dynamics in piezoceramic actuators subject to dynamic-voltage excitations', IEEE Transactions on mechatronics, 2002.

[6] M. Goldfarb and N. Celanovic, 'A lumped parameter electromechanical model for describing the nonlinear behavior of piezoelectric actuators', ASME Journal of dynamc systems, measurement and control, 1997.

[7] S. Chonan, Z. Jiang and T. Yamamoto, 'Nonlinear hysteresis compensation of piezoelectric ceramic actuators', Journal Intell. Mater. Syst. Struct., 1996.

[8] M-S. Tsai and J-S. Chen, 'Robust tracking control of a piezoactuator using a new approximate hysteresis model', ASME Journal of dynamc systems, measurement and control, 2003.

[9] J. G. Smits and W. S. Choi, 'The constituent equations of piezoelectric heterogeneous bimorphs', IEEE Transactions on Ultrasonics, Ferroelectrics and Frequency Control, 1991.

[10] M. Rakotondrabe, Y. Haddab and P. Lutz, 'Plurilinear modeling and discrete μ-synthesis control of a hysteretic and creeped unimorph piezoelectric cantilever', IEEE ICARCV, 2006.

[11] J. Zhong, S. Seelecke, R. C. Smith and C. Büskens, 'Optimal control of piezoceramic actuators', SPIE Smart Structures and Materials, 2003.

[12] S. D. Eppinger and W. P. Seering, 'On dynamic models of robot force control', IEEE ICRA, 1986.

[13] T. S. Low and W. Guo, 'Modeling of a three-layer piezoelectric bimorph beam with hysteresis' IEEE Journal of MicroElectro-Mechanical Systems, 1995.

[14] G. J. Balas, J. C. Doyle, K. Glover, A. Packard and R. Smith, 'μ-analysis and synthesis toolbox', The Mathworks User's Guide-3, 2001.

[15] K. Glover and J. C. Doyle, 'State-space formulae for all stabilizing controllers that satisfy an H_∞-norm bound and relations to risk sensivity', Systems & Control Letters, 1988.

[16] J. C. Doyle, K. Glover, P. K. Khargonekar and B. A. Francis, 'State-space solutions to standard H_2 and H_∞ control problems', IEEE Transactions on Automatic Control, 1989.

[17] B. C. Moore, 'Principal component analysis in linear systems: controllability, observability and model reduction', IEEE Transactions on Automatic Control, 1981.